COMPTON SCATTERING EMISSION IMAGING BASED ON THE V-LINE RADON TRANSFORM AND ITS SIMULATION

R. Régnier[1], M.K Nguyen[1], T.T. Truong[2]

[1]Laboratoire Equipes Traitement de l'Information et Systémes
CNRS 8051/ENSEA/Université de Cergy-Pontoise
F-95302 Cergy-Pontoise Cedex, France
[2]Laboratoire de Physique Théorique et Modélisation
CNRS 8089/Université de Cergy-Pontoise
F-95302 Cergy-Pontoise Cedex, France

regnierremi@yahoo.fr(Rémi Régnier)

Abstract

The Radon transform (RT) on straight lines deals as mathematical foundation for many imaging systems (e.g. X-ray scanner, Positron Emission Tomography) operating only with non-scattered (primary) radiation. Using Compton scattered radiation has turned out to be an attractive alternative to conventional emission imaging. In this paper, we propose a new two-dimensional emission imaging from Compton scattered gamma-rays. Its modeling leads to a Radon transform defined on a pair of half-lines forming a vertical letter V (TV). Moreover we establish the analytic inverse formula of this new TV, which forms the mathematical basis for image reconstruction. Through simulations, image formation and reconstruction results show the feasibility and the relevance of this new imaging. The main advantage is to use a one-dimensional non-moving detector for two-dimensional image reconstruction.

Keywords: Radon transform, image reconstruction, nuclear imaging, tomography, Compton scattering, Biomedical and nuclear imaging modeling

Presenting Author's Biography

Rémi Régnier, M.Sc., is a 2010 graduate of the "École National Supérieur d'Électronique et ses applications", France. He is presently on a research project at the laboratory Équipes Traitement de l'Information et Systèmes under the supervision of professor M.K.Nguyen. His research interest is in the field of modeling and simulation of Compton scattering tomography, inverse problems and generalization of Radon transform

1 Introduction

Radon transforms in the plane [1] (particularly the case of the straight lines) have been extensively studied in the past. These transforms are used to describe imaging processes which do not involve scattered photons. As scattered photons represent 80% of the emitted photons, collecting Compton scattered radiation for imaging purposes [2, 3] has turned out to be an attractive alternative to conventional imaging. In general, scattered radiation acts as noise or disturbance which degrades image quality in imaging modalities working with primary radiation. Collecting emanating scattered radiation for imaging is the new idea which stands opposite to a traditionally admitted view. Extensions of this idea have been advocated in various directions [3]. In three dimensions, image formation modeling leads to the so-called Conical Radon transform (CRT) and this has been supported by numerical simulations [2, 3, 4, 5].

In this paper, we describe the implementation of this idea in two-dimensions. The modeling is achieved by a two-dimensional version of the CRT, called the compound V-line Radon transform (CTV). The simple TV-transform was first proposed by Basko [6] in 1997 as a model for image formation in a two-dimensional Compton camera. However this Basko transform is in fact a V-line Radon transform with swinging axis around a detection site whereas the one considered here has a fixed axis direction. This is the case in many applications, for example two-dimensional structures in biomedical imaging or in material non-destructive testing. One can think of a flat object (or a material slice),which has been turned into an extended gamma ray emitting object. This can be realized by injecting in its bulk medium a radiotracer which, after spreading unevenly throughout the body, emits gamma photons of primary energy E_0. Ideally, Compton scattered radiation is collected by a collimated linear detector and used to reconstruct the primary radiation source distribution of this object (see Fig.1).

In section 2 we present the modeling of the new Compton scattered emission imaging (CSEI) concept which leads to the V-line Radon transform. then we establish its analytic inverse and derive a corresponding filtered back-projection form. This last form has the advantage of reconstructing the image by fast algorithms.

In section 3, we present numerical simulations on image formation and reconstruction for a thyroid and a Shepp-Logan phantoms to support the feasibility of this new imaging. We show the main results on these simulations. The paper ends with a short conclusion on the obtained results and opens some future research perspectives.
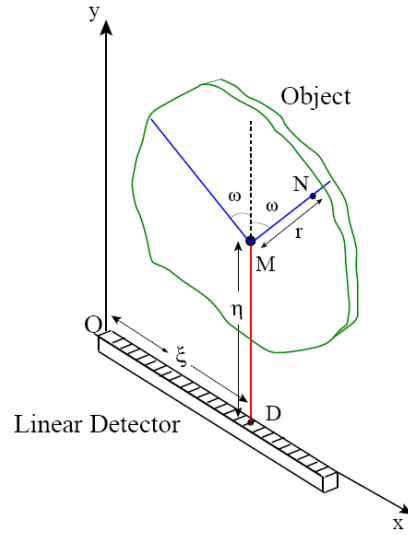

Fig. 1 Experimental setup for the detection of the photons and parameters used in the mathematical theory

2 Modeling of the Compton scattered emission imaging (CSEI) and the V-line Radon transform

2.1 Image formation modeling

For tomographic emission imaging, we consider a 2D-object containing a non-uniform radioactivity source distribution, which is represented by a non negative continuous function $f(x, y)$ with bounded support. A collimated linear detector collects only outgoing radiation from the object which is parallel to the direction of the collimator holes (Fig.1).

If the detector is set to absorb gamma photons at energies below E_0, the energy of primary photons, the photons have undergone a Compton scattering at a site **M** in the bulk of the object under a scattering angle ω. We neglected higher order scattering which occurs with a much smaller probability.

The photon flux density measured at a detecting site **D** is due to the sum of scattered radiation flux densities outgoing from the set of scattering sites lying along the axis of the collimator at **D**. As scattered photons have energy E, they have been deflected from an incident direction by a scattering angle ω, related to E by the Compton formula :

$$E = \frac{E_0}{1 + \frac{E_0}{mc^2}(1 - cos(\omega))} \tag{1}$$

where $mc^2 = 0.511$MeV.

Thus the totality of the deflected density flux, for each scattering site **M**, is due to the sum of all point sources

lying on the V-line with **M** as vertex.

We use cartesian coordinates in Fig.1 , and call $g(\xi, \omega)$ the measured photon density flux at **D** under the scattering angle ω . We can write $g(\xi, \omega)$ as the sum over all sites **M** lying on a line parallel to the collimator hole at a detection site of $TVf(\xi, \eta, \omega)$

$$g(\xi, \omega) = K(\omega) \int_0^\infty \frac{d\eta}{\eta} TVf(\xi, \eta, \omega), \qquad (2)$$

where $K(\omega)$ contains the square of the classical electron radius, the average electron density and the Klein-Nishina scattering probability function

and where

$$TVf(\xi, \eta, \omega) = \int_0^\infty \frac{dr}{r} f(\xi + r\sin(\omega), \eta + r\cos(\omega))$$

$$+ \int_0^\infty \frac{dr}{r} f(\xi - r\sin(\omega), \eta + r\cos(\omega)),$$
$$\qquad (3)$$

this is the V-line Radon transform of the unknown activity distribution $f(x, y)$. This is the reason why equation (2) is called the compound V-line Radon transform (CTV) of $f(x, y)$. We shall study first the V-line Radon transform given by equation (3).

2.2 Definition of the Radon transform on a V-line (TV)

In the last integral, $f(x, y)$ is integrated on a discontinuous line having the form of the V-line with a symmetry axis parallel to a fixed direction. Thus image formation by Compton scattered radiation in two dimensions leads to a new concept of a Radon transform on a V-line. A simple case of the V-line Radon transform is obtained when $\eta = 0$.

This simplification is in fact the imaging process of a ideal collimated one-dimensional Compton camera. Primary radiation emitted from the object bulk is scattered by a linear scattering detector, which lies along the Ox-axis of a cartesian coordinate system and absorbed just on a next layer along the vertical direction by a second absorbing detector.

The V-line Radon transform $TVf(x, y)$ is defined as an integral of the function $f(x, y)$ with $\eta = 0$ in equation (3). The factor $1/r$ (resp. $1/r^2$) in the integrand accounts for the photometric law of photon propagation in two dimensions (resp. in three dimensions). From now, on $K(\omega)$ is included in the definition of f to keep the writing simple. Under the change of variables $t = tan(\omega)$ and $z = rcos(\omega)$, equation (3) reads

$$g(\xi, t) = \int_0^\infty \frac{dz}{z} \left[f(\xi + tz, z) + f(\xi - tz, z) \right]. \quad (4)$$

The TV of a given point source (x_0, y_0) : when $f(x, y) = \delta(x - x_0)\delta(y - y_0)$ in equation (4) $g(\xi, t)$ is the sum of two Dirac delta distributions, which have a support in the upper (t, ξ)-plane, consisting of two half-lines, with $t > 0$, meeting at $\xi = 0$ on the ξ-axis and having a slope $\pm y_0^{-1}$, ie :

$$t = \left| \frac{x_0 - \xi}{y_0} \right|, \text{ so } \omega = arctan \left| \frac{x_0 - \xi}{y_0} \right|. \qquad (5)$$

Thus in a (ω, ξ)-representation, this is just an arctan-curve.

2.3 Inverse formula TV^{-1}

The inverse transform TV^{-1} can be worked out using Fourier transform $\tilde{f}(q, \omega)$ (resp. $\tilde{g}(q, \omega)$) with respect to the variable x (resp (ξ)) in $f(x, y)$ (resp. $g(\xi, \omega)$).

$$g(\xi, \omega) = \int_{-\infty}^\infty dq \tilde{g}(q, \omega)e^{2i\pi q\xi} \qquad (6)$$

and

$$f(x, y) = \int_{-\infty}^\infty dq \tilde{f}(q, y)e^{2i\pi qx}. \qquad (7)$$

Then equation (6) becomes

$$\tilde{g}(q, \omega) = 2 \int_0^\infty \frac{dz}{z} \tilde{f}(q, z)cos(2\pi qzt). \qquad (8)$$

Equation (8) then appears as a cosine-Fourier transform of $\tilde{F}(q, z) = \tilde{f}(q, z)/z$

$$\tilde{g}(q, t) = 2 \int_0^\infty dz \tilde{F}(q, z)cos(2\pi qzt). \qquad (9)$$

Thus using the invertibility of the cosine transform, we can obtain

$$\tilde{f}(q, t) = 2 |q| \int_0^\infty dt \tilde{g}(q, t)cos(2\pi qzt). \qquad (10)$$

Performing the Fourier inverse transform we can recover $f(x, y)$ which can be expressed as the result of an integral transform (TV^{-1}) with the kernel [7]:

$$k(w, z \,|\xi, t) = \frac{-z}{2\pi^2} \left[\frac{1}{(x - \xi + zt)^2} + \frac{1}{(x - \xi + zt)^2} \right],$$
$$\qquad (11)$$

This is to be understood as a generalized function, or distribution.

To establish the inverse transform of the CTV, we can consider it as a TV transform of the following function

$$L(\xi, \omega) = \int \frac{d\eta}{\eta} f(\xi, \eta, \omega), \qquad (12)$$

which can be viewed as a convolution product between the Fourier transform of $1/\eta$ and the Fourier transform of $f(\xi, \eta, \omega)$, as a function of η. Thus the inverse of the CTV is the product of a deconvolution in the dual variable to η times TV^{-1}. These two steps lead to a rather involved analytic expression, which does not lend itself to accurate numerical treatment. So we choose to construct a new filtered back-projection method for image reconstruction which has the advantage of offering fast algorithms. This is done in the next section.

2.4 Inversion method by filtered back-projection(FBP-IM)

Let us recall that the most popular inversion method of the Radon transform is so-called *filtered back-projection method*(FBP), due to its similarity to the one of standard Radon transform, but the novelty is that the FBP is carried on the V-lines but not on the straight lines.

In the Radon transform, the FBP is an exact inversion formula by combining the action of the ramp filter and the back-projection operation. We now derive the FBP for the TV.

Technically the back projection principle consists in assigning the value $g(\xi, \omega)$ to every point on the "projection" V-line, which has given rise to this value, and then to sum over all contributions for every V-line "projection". More precisely, the back-projection at angle ω in (x,y) is the sum of projections at angle ω at the points $\xi_1 = x + y\tan\omega$ and $\xi_2 = x - y\tan\omega$, where (x,y) is projected :

$$R_\omega(x,y) = g(x+y\tan\omega, \omega) + g(x-y\tan\omega, \omega). \quad (13)$$

The back-projection of every projection defines the back-projection operator $TV^\#$ which is obtained by summing over every angle ω. Here a y-factor appears because of dr/r in the definition of the projections (3).

Now the action of the ramp filter operator Λ over a function $f(x,y)$ in the first variable of a function $f(x,y)$ in the first variable is defined in Fourier space by $\Lambda \tilde{f}(q,y) = |q| \, \tilde{f}(q,y)$, where the Fourier transform is taken on x. From equation (10) we have

$$f(x,y) = y \int_0^\infty (\Lambda g)(x+ty, t) + (\Lambda g)(x-ty, t))dt. \quad (14)$$

In terms of the angle ω, the inversion formula reads:

$$f(x,y)y = y^2 \int_0^{\pi/2} \frac{d\omega}{\cos^2\omega} \left[(\Lambda g)(x + y\tan\omega, \omega) \right.$$
$$\left. + (\Lambda g)(x - y\tan(\omega), \omega)\right]. \quad (15)$$

Defining the operator M_ω as

$$M_\omega g(\xi, \omega) = \frac{g(\xi, \omega)}{\cos^2\omega} \quad (16)$$

and knowing that

$$TV^\# g(x,y) = \frac{1}{y} \int_0^{\pi/2} d\omega \left[g(x + y\tan\omega, \omega) \right.$$
$$\left. + g(x\tan\omega, \omega)\right]. \quad (17)$$

We recover the original density f(x,y) by a filtered-back projection

$$f(x,y) = y^2 \left(TV^\# M_\omega \Lambda TV f\right)(x,y). \quad (18)$$

This filtered-back projection inversion on V-lines, obtained for the first time, generalizes the one known in the standard Radon transform on straight lines. The reconstruction formula (18) is mathematically equivalent to the reconstruction by TV^{-1} of the previous subsection. But the advantage of the filtered back-projection inversion formula is that it may be implemented by fast algorithms.

3 Numerical simulations

3.1 Simulation of the V-line Radon transform

We present now numerical simulations of the TV transform of different geometrical objects. The algorithms have been implemented with MATLAB. Many parameters play an important role in the numerical implementation of the TV transform such as the distance between the source and the detector, the angular sampling rate, the dimension of the detector and the spatial sampling rates. The quality of the reconstructions depends of course on these parameters (problems of discretization and interpolation) as well as on the geometry of the objects under study. The projection gives us the value of the photon density flux on the points of the detector according to the scattering angle (corresponding at the energy of photons). In view of the discretized image, it is important to make good interpolation to match the data matrix of pixels.

We present now the results of numerical simulations. The original images (Fig.2, 5) of size 512×512 of length units represent respectively a thyroid with small nodules phantom and a Shepp-Logan phantom. Fig.3 and 6 show the TV transform of the phantoms with angular sampling rate $d\omega = 0.005$ rad and 314 projections ($\pi/2/0.005 = 314$) which are the images of Compton scattered radiation on the camera in terms of the distance ξ and the scattering angle ω.

We note that the shape of the V-line Radon transform (or the shape of the projections) in the (ω, ξ)-representation is consistent with the arctan-curve (Fig.3, 6 and see equation (5)). It is observed that the large values of the V-line Radon transform are obtained at the small scattering angles and vice versa. Thes results are consistent with the physical phenomenom of scattering (at the large ω, the Klein-Nishina probability decreases rapidly) and the photon density flux is inversely proportional to the distance source-detector (r), hence proportional to $\frac{1}{r}$. (Fig.3, 6)

3.2 Difficulties of simulation of the analytic inverse transform TV^{-1}

The simulation of the analytic inverse formula poses a real mathematical challenge to overcome. In fact the kernels (equations (9,10)) of the integrals are singular. Moreover integration boundaries of these integrals are at infinity. So several problems of discretization and interpolation arise. We choose the inversion method by filtered back-projection (FBP) because it gives the satisfactory results in reasonably computational time. Moreover it is proved that the FBP is equivalent to the inverse transform TV^{-1}.

3.3 Filtered back-projection

The reconstruction is performed using the filtered back-projection inversion method (FBP) of the TV-transform. However, back-projection on V-lines generates more artifacts than back-projection on straight lines in standard two-dimensional Radon transform, due to the existence of more spurious line intersections. In order to reduce these artifacts, the Hann filter H is used. It is defined on the Fourier domain by its action on the first variable of a function f as follows :

$$\tilde{H}f(q, y) = \frac{|q|}{2}(1 + cos(2\pi q))\tilde{f}(q, y), \qquad (19)$$

where the Fourier transform is taken on the first variable. The reconstruction quality shows the feasibility of this imaging modality.

The reconstructions using FBP are given in Fig.4 and 7. The artifacts are due to the limited number of projections. A choice of a smaller $d\omega$ would improve image quality. But when the number of projections is about equal to the number of pixels the reconstruction quality is stable. In order to qualify the reconstruction quality we use the mean square error (MSE) which is defined as :

$$MSE = \frac{(Image_{original} - Image_{reconstructed})^2}{Number_{pixels}}. \qquad (20)$$

We obtain the MSE $= 2.8 * 10^{-3}$ for $d\omega = 0.005$ rad and the MSE $= 2 * 10^{-3}$ for $d\omega = 0.0025$ rad (twice smaller than the previous case) (Fig.7, 8). This shows the robustness of the proposed method.

These results illustrate undoubtedly the feasibility of the new imaging modality, for which the main advantage resides in the use of a one-dimensional non-moving Compton camera for two-dimensional image processing, see Fig.1.

4 Conclusion

In this paper, we present a new Compton scattering tomography, its modeling and simulations with the help of a novel class of Radon transform defined on a discontinuous line having the shape of a V letter. We show that its analytic inverse transform poses some difficulties for numerical simulations. Fortunately, this transform is equivalent to filtered back-projection inversion method for which numerical simulations turn out to be efficient. Finally the simulation results support the feasibility and the relevance of the new proposed imaging in which the main advantage resides in the two-dimensional image reconstruction from scattered radiation collected by a one-dimensional collimated non-moving camera.

Furthermore, the extension of the V-line Radon transform to a family of cones with swinging axis around a site in the space corresponding to a gamma camera without mechanical collimator, poses a real mathematical challenge to overcome in the future.
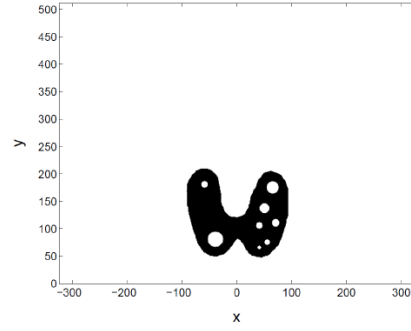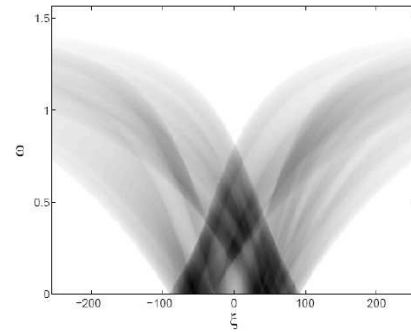

Fig. 2 Original thyroid phantom

Fig. 3 The TV transform of the thyroid image shown in Fig. 2 with $d\omega$ =0.005 rad, the arctan form of this result is consistent with the mathematical theory.
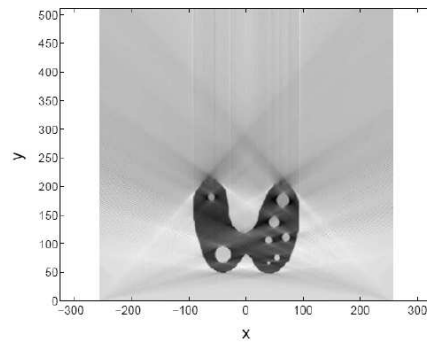

Fig. 4 FBP-IM reconstruction of the thyroid image with $d\omega$ =0.005 rad, the small structures in the object are clearly reconstructed.
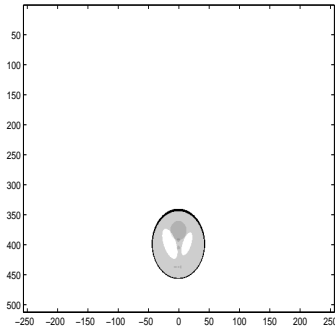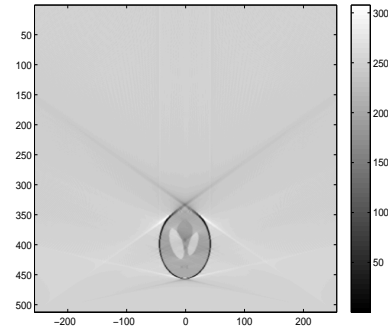
Fig. 5 Original Shepp-Logan phantom

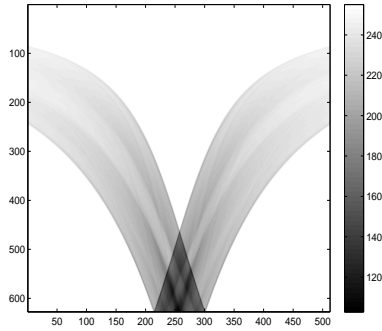Fig. 7 FBP-IM reconstruction of the Shepp-Logan image with $d\omega$ =0.005 rad.

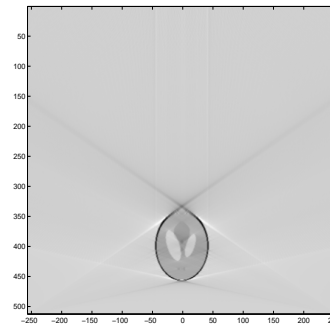Fig. 6 The TV transform of the Shepp-Logan image shown in Fig. 5 with $d\omega$ =0.005 rad.

Fig. 8 FBP-IM reconstruction of the Shepp-Logan image with $d\omega$ =0.0025 rad, the quality is slightly improved compared to Figure 7.

5 References

[1] J. Radon. Über die bestimmung von funktionnen durch ihre integralwerte längs gewisser mannigfaltikeiten. *Ber.Verh.Sachs.Akad.Wiss.Leipzig-Math.Natur.Kl.*, 69:262–277, 1917.

[2] M.K. Nguyen and T.T. Truong. On an integral transform and its inverse in nuclear imaging. *Inverse Problems*, 18:265–277, 2002.

[3] M.K. Nguyen T.T. Truong, H.D. Bui and J.L. Delarbre. A novel inverse problem in γ-rays emission imaging. *Inverse Problems in Science and in Engineering*, 12:225–246, 2004.

[4] M.K. Nguyen T.T. Truong, C. Driol and H. Zaidi. On a novel approach to compton scattered emission imaging. *IEEE Transactions in Nuclear Sciences*, 56:1430–1437, 2009.

[5] T.T. Truong M.K. Nguyen and H. Zaidi. The mathematical foundation of 3d compton scatter emission imaging. *International journal of Biomedical Imaging, Special Issue on Mathematics in Biolodical Imaging*, doi : 10. 1155/2007/92780,2007.

[6] R. Basko G.L. Zeng and G.T. Gullberg. Analytical reconstruction formula for the one-dimensional compton camera. *IEEE Trans. Nucl. Sci*, 44:1342–1346, 1997.

[7] M.Morvidone M.K. Nguyen, T.T. Truong and H.Zaidi. A novel v-line radon transform and its imaging applications. In *International Journal of Biomedical Imaging, Special issue on Mathematical methods for Images and Surfaces*, 2010.

[8] H.H. Barrett. The radon transform and its applications. *Progress in Optics*, 21:219–286, 1984.

[9] E.L. Ginzton. Quasi fast henkel transform. *Optics letters*, 1(1), 1977.

[10] J.L. Delarbre M.K. Nguyen, T.T. Truong and J.L. Starck. Modeling and simulation for scattered gamma-ray imaging. In *Proc. 5th EUROSIM congress on Modeling and Simulation*, Marne la Valle, France September 2004.

[11] C. Driol M.K. Nguyen and T.T. Truong. Modeling and simulation results on high sensitivity scattered gamma-ray imaging. In *Proc. 6th EUROSIM congress on Modeling and Simulation*, September 2007.